Proceedings of the 4th World Congress on Momentum, Heat and Mass Transfer (MHMT'19)
Rome, Italy – April, 2019
Paper No. ICMFHT 126
DOI: 10.11159/icmfht19.126

Improving Separation Efficiency of Particle less than 10 Microns in Hydrocyclone

Adebola Adewoye[1], Mamdud Hossain[1], Sheikh Zahidul Islam[1], Aditya Karnik[1]
[1]Robert Gordon University
Garthdee Road, Aberdeen, United Kingdom
j.a.adewoye@rgu.ac.uk; m.hossain@rgu.ac.uk; s.z.islam1@rgu.ac.uk; a.karnik@rgu.ac.uk

Abstract **-** Hydrocyclone separate oil droplet size of 15µm and above from oil-water emulsion, particles less than 15µm are difficult to separate using hydrocyclone. The aim of this paper is to improve the separation efficiency of oil particles size of less than 10 µm in hydrocyclone. This paper evaluates the use of ferromagnetic particles for improving separation efficiency of droplet size less than 10µm in liquid-liquid hydrocyclone. Eulerian-Lagrangian model was used in conjunction with the Reynolds Stress Model (RSM) for turbulence and Magneto Hydrodynamic model (MHD) account for ferromagnetic particle conductivity. It was observed that use of magnetic particles increases separation efficiency by approximately 30% and 22% for 0.018% and 0.18% feed concentration respectively for particle size between 1-10µm and 32% increment was observed for particle size between 11-15µm. The increment is attributed greatly to the increase in density of oil as a result of doping micro-sized magnetic particles with oil-emulsion. Finally, it was seen that increasing magnetic field strength from 0.5 Telsa to 1.5 Telsa increases separation efficiency in the range of 1-4% and the use of magnetic particles increase the velocities of the fluid.

1. Introduction

Produced water is a major by-product in the oil and gas industry, it is estimated that approximately 14 billion bbls [1] of water are produced annually. Oil in water exists in three different forms; dissolved, dispersed and free oil; dissolved oil has a droplet size of 150µm or larger and can be separated easily via gravity. The dispersed oil (emulsion) on the other hand has smaller oil droplet size ranging from 0.5-80µm making the separation more difficult. In separating the dispersed oil from produced water, hydrocyclone is usually the preferred choice of equipment [2].

Hydrocyclone operates by fluid entering the cyclone tangentially via the inlet opening into the cylindrical section creating a swirling flow (vortex); the swirling flow generates a high centrifugal force required to separate the oil; therefore, higher density fluid (water) centrifuge to the wall of the cyclone whereas the lesser density fluid (oil) migrates towards the core of the cyclone. Hydrocyclone generally separate oil droplet size of 15µm and above from produced water, particles less than 15µm are difficult to separate using hydrocyclone as the separation efficiency of hydrocyclone decrease with particle size [3]

Geometry and operating parameters have been used by many researchers in the optimization of hydrocyclone separation efficiency. Noroozi [4] used helical inlet to increase separation efficiency by 10% while increased inlet diameter as well was found to have also increased the separation efficiency of hydrocyclone [5] [6]. Research has also shown that Larger cone angle decreases separation efficiency [7], larger underflow diameter lower separation efficiency [8] [5] and increased overflow diameter decreases the separation efficiency [5] [8]. Some researchers have looked at the use of smaller diameter hydrocyclone to improve efficiency [9] [10] [11] while another researcher had some improved efficiency by changing the conical section of the hydrocyclone to hyperbolic and parabolic shape [12]. All the journals reviewed for geometry parameter have one thing in common; droplet size of efficiency as reviewed is 10µm and above which has led to the conclusion that changes in geometrical dimension alone have a great effect on large particles collection/separation and little effect on finer particles [13].

Siadaty [13] used a new approach of separating fine solid particles of 2-4µm from gas using hydrocyclone. The separation efficiency increased by 8% and 2% for 2µm and 4µm respectively by applying an external magnetic field. A magnetic cyclone was first developed in the late sixties with the aim of providing an additional external force to supplement gravitational and centrifugal forces that cause classification and separation of solid-liquid [14]. Watson and Fricker both

proposed design for separation of ferromagnetic solid from liquid in hydrocyclone in 1983 and 1985 respectively [15]. In Watson proposed design, the magnetic force is outward and attract particles to underflow while in Fricker proposed design, the magnetic force is inward, and particles are attracted to the overflow. Freeman [16], Premaratne [14], Fan [17] used magnetic hydrocyclone to improve separation efficiency of solid particles (10μm and above) by approximately 5-7% more than conventional hydrocyclone (hydrocyclone without magnetic magnetism).

Mirshahghassemi [18]; Juan [19]; and Riele [20] used magnetic force to separate oil from water by mixing oil emulsion with ferromagnetic nanoparticles coated with polymers (thermoresponsive polymer). Exerting magnetic field to oil emulsion doped with polymer coated nanoparticles induced migration of polymer coated nanoparticles to the wall thereby separating oil attached to polymer coated nanoparticles. After separation, a slight increase in temperature is required to detach oil from polymer coated nanoparticles. This principle is applied in the current studies to improve the separation of oil droplet from water in conjunction with the use of Watson magnetic hydrocyclone design.

According to Shen [15], in magnetic hydrocyclone; only centrifugal, drag and magnetic force have a significant effect on the separation efficiency. The principle is similar to a conventional cyclone where the direction of particle motion/separation is affected by the total forces acting on the particle [21] [22]. Centrifugal and drag forces are proportional to the magnitude of tangential and radial velocities while the magnetic force is influence by ferromagnetic material used and magnetism induced into the flow.

1.1. Present Work

The aim of this paper is to evaluate the use of ferromagnetic particles for separation of droplet size of less than 10μm in liquid-liquid hydrocyclone and the overall effect of ferromagnetic material on cyclone separation. It was assumed that a micron-sized Ferromagnetic material [23] with selected surfactants was added to the oil-water emulsion before feeding the emulsion into the cyclone. Addition of surfactants make magnetic particle to be oleophilic and hydrophobic in nature thus attraction of oil to the surface of ferromagnetic material; magnetic particles induce magnetism into the fluid to enable magnetic attraction and increase the density of oil for better separation.

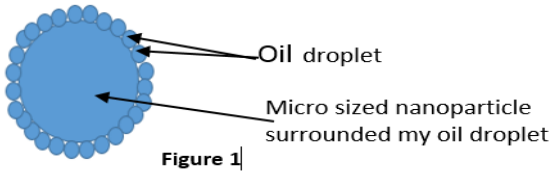

Fig. 1: Dropping of Oil droplet.

The separation efficiency, velocities, and effect of concentration in a cyclone with and without magnetic particle were assessed. CFD Eulerian-Lagrangian model was used for the evaluation, Discrete Phase Model (DPM) was used to model the discrete phase, Reynold Stress Model (RSM) was used to model the turbulence while magnetism was introduced into the system using of Magneto-Hydrodynamic model (MHD). The particles were assumed to be spherical and the flow laminar to the particles

2. Numerical model

Continuity Equation

The rate at which mass enters a system is equal to the mass out of the system plus accumulated mass in the system. For an unsteady three-dimensional incompressible fluid, the density of fluid remains constant and the continuity equation is given by equation 1

$$\nabla . u = 0 \tag{1a}$$

Equation of mass conservation is

$$\frac{\partial \rho}{\partial t} + (\nabla . u)\rho = 0 \tag{1b}$$

Momentum Equation

Change of momentum of a fluid particle equals the sum of the forces on the particle (Newton Second Law). Therefore for an incompressible particle at a point with x, y,z directions, the rate of increase of the momentum (in x,y,z directions) per unit volume is given by equation 2 (a-c)

$$\frac{\partial(\rho u)}{\partial t} + \nabla.(\rho u U) = -\frac{\partial p}{\partial x} + \nabla.(\mu \nabla u) \tag{2a}$$

$$\frac{\partial(\rho v)}{\partial t} + \nabla.(\rho v U) = -\frac{\partial p}{\partial y} + \nabla.(\mu \nabla v) \tag{2b}$$

$$\frac{\partial(\rho w)}{\partial t} + \nabla.(\rho w U) = -\frac{\partial p}{\partial z} + \nabla.(\mu \nabla w) \tag{2c}$$

2.1. Reynold Stress Model (RSM)

RSM is a seven-equation model which transport Reynold stresses, these equations are given below. RSM closes the RANS equations by solving the individual Reynold stresses and all mean flow properties together with an equation for the dissipation energy.

$$\frac{DR_{ij}}{Dt} = \frac{\delta R_{ij}}{\delta t} + C_{ij} = -D_{T,ij} + D_{L,ij} - P_{ij} - G_{ij} + \emptyset_{ij} + \varepsilon_{ij} + F_{ij} \tag{3a}$$

$\frac{\delta R_{ij}}{\delta t}$ −Reynold stresses transport equation
C_{ij} −Stress by convection
$D_{T,ij}$ −Turbulence Diffusion term
$D_{L,ij}$ −Transport of Reynold stress by Molecular
P_{ij} −Stress Production term
G_{ij} −Buoyancy production
$\emptyset_{ij}$ −Pressure Strain
ε_{ij} − Dissipation term/ Rate of dissipation
F_{ij} −Production by system rotation

$$\varepsilon_{ij} = \frac{2}{3}\delta_{ij}(\rho\varepsilon + Y_m) \tag{3b}$$

Y_m =Dilatation dissipation and is used for compressible fluid therefore ignored for this simulation
ε = Scalar dissipation and given by equation 3c below

$$\frac{\partial}{\partial t}(\rho\varepsilon) + \frac{\partial}{\partial x_i}(\rho\varepsilon u_i) = \frac{\partial}{\partial x_j}\left[\left(\mu + \frac{\mu_t}{\sigma_\varepsilon}\right)\frac{\partial \varepsilon}{\partial x_j}\right] C_{\varepsilon 1}\frac{1}{2}[P_{ii} + C_{\varepsilon 3}G_{ii}]\frac{\varepsilon}{k} - C_{\varepsilon 2}\rho\frac{\varepsilon^2}{k} + S_\varepsilon \tag{3c}$$

2.2. Lagrangian Particle Tracking Model

The Lagrangian discrete phase model (DPM) was used to model the discrete phase, the model is used for dilute medium density particle concentration in flows. The acceleration of the particles is given by Newton's second law

$$\frac{d}{dt}u_p = \sum f_p \tag{4a}$$

Where $f_p = {}^{F}/_{m_p}$ denotes the forces per mass on a particle, therefore equation 6 can be written as

$$\frac{d}{dt}u_p = F_D(u - u_p) + \frac{g_x(\rho_p - \rho)}{\rho_p} + F_x \tag{4b}$$

F_x is the additional particle forces which include virtual mass force, saffman lift force, pressure gradient force, Magnus force and basset force; these forces but will be ignored for this study because of the effect of magnetic particle and magnetic force.

u - fluid phase velocity, u_p- particle velocity, ρ-fluid density, ρ_p -the density of the particle

Drag Force F_D

Drag force is based on the velocity difference between particles and fluid and it is expressed by

$$F_D = \frac{18\mu}{\rho_p d_p^2}\frac{C_D R_e}{24} \tag{4c}$$

$$R_e = \frac{\rho d_p |u_p - u|}{\mu} \tag{4d}$$

Where u= fluid phase velocity, u_p =Particle velocity, μ = Molecular Viscosity, ρ = Density of Fluid, ρ_p = Density of Particle, d_p = Particle Diameter, R_e = Reynold number, $C_D = Drag\ Coefficien$t

2.3. Magnetohydrodynamic Model (MHD)

MHD studies magnetic properties and behaviour of electrically conducting fluids; typical governing equation for MHD are fluid dynamics and Maxwell equation. The electrically conductive fluid is usually the discrete phase; thus oil droplet is the conductive fluid used in this study. For a conductive fluid, the Magnetic induction equation is shown in equation 5a below

$$\frac{\partial B}{\partial t} = \nabla(u.B) - \nabla(\eta \nabla B) \tag{5a}$$

where $\eta = \frac{1}{\mu\sigma}$

B =Magnetic Field in Tesla u = Fluid velocity Field μ=Magnetic Permeability

η =Magnetic Diffusivity ∇= Operator referred to as grad, nabla, or delta σ =conductivity of fluid

Fluid carrying current density in a magnetic field experience Lorentz force (F_m) per unit volume given by equation 5b

$$F_m = -\nabla\left(\frac{B^2}{2\mu}\right) + \frac{1}{\mu}B.\nabla B \tag{5b}$$

3. Hydrocyclone Simulation

The diameter of the cylindrical section of the cyclone and length of cylindrical parts was 75mm, inlet dimension 22.16mm x 22.16mm, Vortex finder diameter 25mm, the insertion depth of vortex finder: 50mm, Diameter of Spigot 12.5mm 12.5mm and cone angle 20^{o}. This geometry is in accordance with Hseih [24].

3.1. Solution Technique

To reduce computational time and achieve a good result, hexahedral structured mesh with 348546 elements was used. Discretization of continuity and momentum equations was solved using pressure-based solver. The pressure-velocity was coupled using SIMPLE, spatial discretization evaluated using Least Square Cell Based and pressure, momentum, turbulence kinetic energy, turbulence dissipation rate and magnetic field in the x,y and z directions all discretized using second-order upwind models. The time steps were set to 0.001s for a steady state simulation.

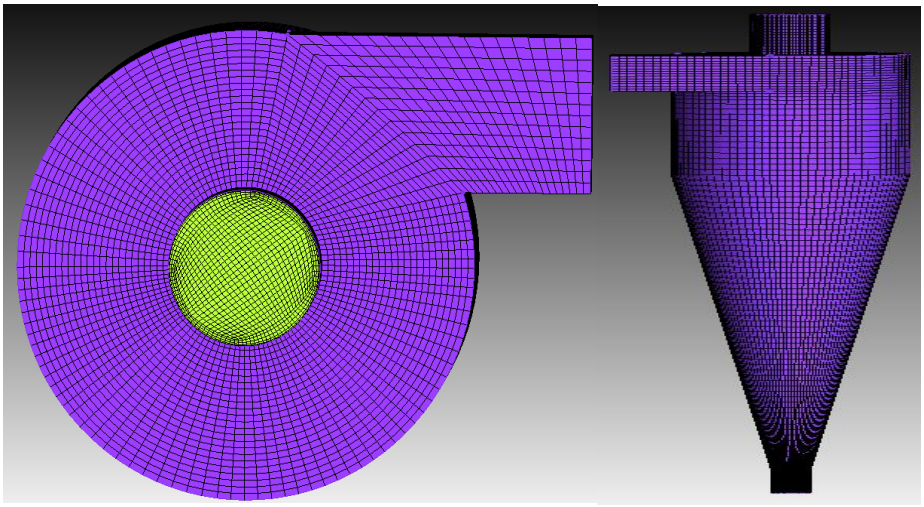

Fig. 2: Hydrocyclone Mesh.

3.2. Operating Conditions

The simulation was carried out using inlet velocity of 2.5m/s, at differents oil-water concentration of 0.018%, 0.18%, 1.8% and 18%. Diesel Oil with a density of 780kg/m^3 was used for the simulation and water density was assumed to be 1000kg/m^3. The vortex finder (overflow) and spigot (underflow) of the cyclone were exposed to the atmosphere, therefore, the gauge pressure was set to 0 atm. The density of magnetic particle was assumed to be 5175kg/m^3

Magnetic particles of size lightly higher than oil droplet to be separated was assumed to have been treated with surfactant and mixed with the oil emulsion, oil droplets are expected to attract to the surface of the magnetic particle, therefore, doping the magnetic particle (applicable for oil droplet less than 10µm). For bigger oil droplet size, magnetic particle is attracted to the surface of the oil droplet.

The approach of Watson magnetic hydrocyclone [15] was used for the current study.

4. Results and Discussion of Results

4.1. Effect of magnetic Particle on oil-water separation efficiency.

The grade efficiency in figure 3, 4 and 5 was obtained by means of stochastic particle tracking. It can be seen from figures 3(a-d) that magnetic particles increase the separation efficiency of oil from water when compared with hydrocyclone without magnetic particles (conventional cyclone).

From figure 3a and 3b, it was observed that use of magnetic particles increases separation efficiency by up to 30% and 22% for 0.0007kg/s (0.018%) and 0.007kg/s (0.18%) mass loading respectively for particle size between 1-10µm. Up to 32% increment was observed for particle size between 11-15µm. Above 15µm decrease in efficiency was noted. Improved

efficiency is attributed partly to the increase in density of oil as a result of adding micro-sized magnetic particles to oil emulsion. Density change is due to doping of oil particles on the surface magnetic particles, therefore, making the density doped particles to be more than that of water. This means doped oil droplets will move to the wall during separation and discharged via the underflow as opposed to the discharge of oil droplet from the overflow in a conventional deoiling hydrocyclone.

Figure 3a and 3b further show the increase in efficiency of magnetic cyclone close-up as the particle size increases and at about 56µm (figure 3a) the efficiency of conventional cyclone becomes higher than that of Magnetic cyclone. The reduction in separation efficiency of magnetic cyclone shows that the use of magnetic cyclone will benefit smaller droplet than larger droplets.

Figure 3(a-d) show that magnetic cyclone efficiency curve has a more pronounced fish hook (unevenness of graph) effect than conventional cyclone. Fishhook is prominent when the particle size is less than 15µm [25] and this reflects in figure 3c and 3d. This is attributed to droplets interaction, as droplets move to the wall of the cyclone, particles coalesce to form bigger droplets and smaller droplets are entrained by the wake region behind the large droplets and are carried to the overflow

The cause of fishhook effect is credited to entrainment in the wake flow, reduction of drag force and change in the resultant force direction for the fine particles [25]; centrifugal, drag and magnetic forces are the most prominent forces in this magnetic hydrocyclone, affecting the resultant force. Lines of best fit for each of the graphs can be drawn to reduce appearance of fish hook as shown in Figure 3e.

Figure 3d shows that with an increase in the external magnetic field, the efficiency increases slightly by about 1-4%, this shows that Magnetism is not the major contributor to the increase in separation efficiency of oil emulsion rather the use of a micro-sized magnetic particle which created higher density differential between the fluid.

Fig. 3a: Oil Concentration of 0.018% (0.0007Kg/s).

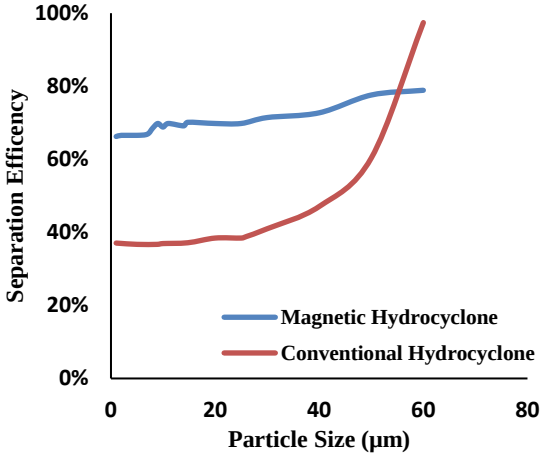

Fig. 3b: Oil Concentration of 0.18% (0.007Kg/s).

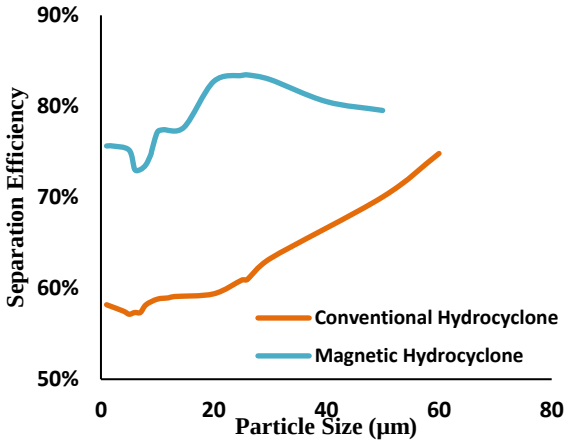

Fig. 3(a-b): Comparison of Separation Efficiency of magnetic hydrocyclone and conventional hydrocyclone

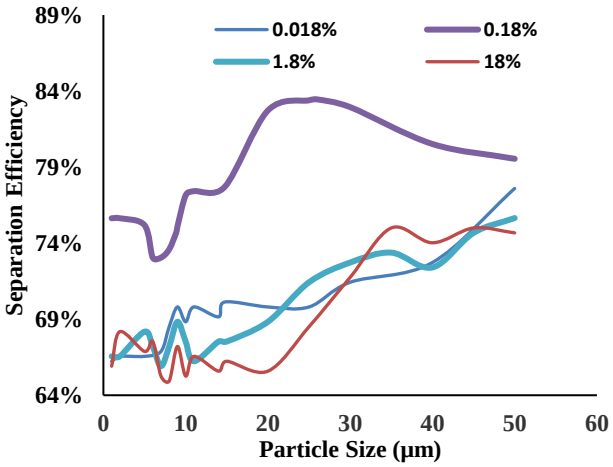

Fig. 3c: Effect of Concentration on Magnetic Hydrocyclone Separation.

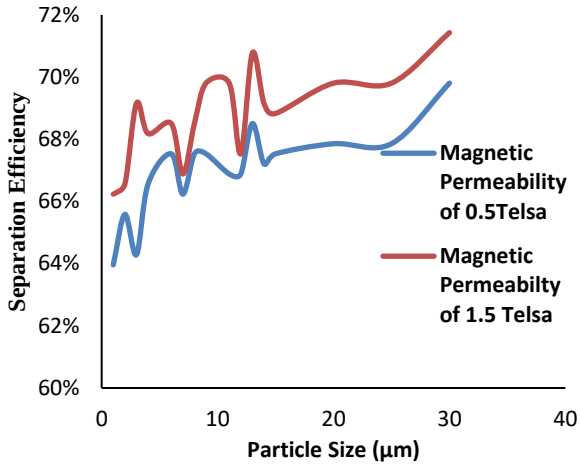

Fig. 3d: Effect of External Magnetic field on Separation Efficiency of Magnetic Hydrocyclone.

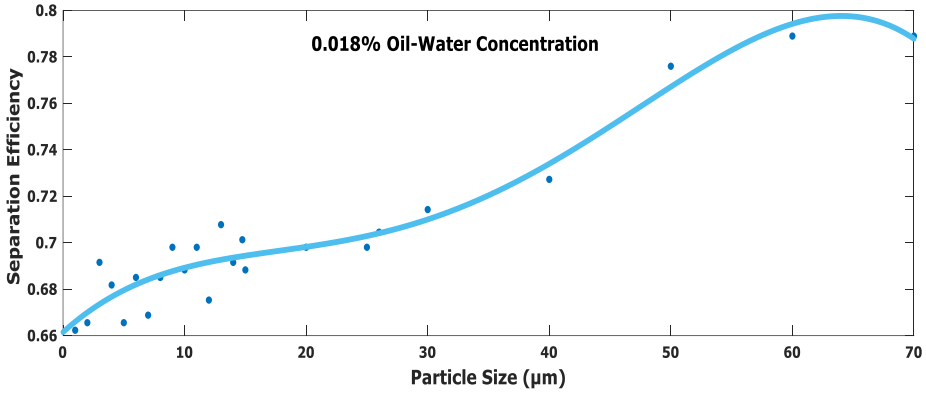

Fig. 3e

4.2. Effect of Droplet Concentration in the Separation Efficiency of Magnetic Hydrocyclone

It can be seen from figure 4a for conventional hydrocyclone that as concentration increases from 0.018% to 0.18%, the separation efficiency increases from approximately 37% to 59%. The efficiency further increases to about 67% when the concentration was increased to 1.8%. With a further increase in concentration to 18%, separation efficiency dropped to about 35% for 10µm oil droplet size. The same trend can be seen for all the particle sizes observed. This indicates that increasing concentration for greater efficiency is restricted to a certain value where maximum separation is achieved and a further increase will cause a decrease in separation efficiency, in this study the optimal concentration is 1.8%. From literature concentration of discrete phase in hydrocyclone most not be more than 10% for optimal efficiency.

In Magnetic hydrocyclone (figure 4b) as concentration increase from 0.018% to 0.18% efficiency increase from 69% to 77%. The efficiency, however, decreases to 67% and 65% when the concentration was increased to 1.8% and 18% respectively. Other particles sizes follow the same trend as shown in figure 4b. This also indicates that increasing concentration for greater efficiency is restricted to a certain value where maximum separation is achieved and a further increase will cause the decrease in separation efficiency, in this study the optimal concentration is 0.18%. This shows that for optimum use of magnetic hydrocyclone, the concentration of the dispersed phase must be relatively small. In general, high concentration leads particle-particle interaction which reduces settling velocities, lower swirling and hindered settling effect / centrifugal force thus reduces separation efficiency [26].

Fig. 4a: Conventional Hydrocyclone.

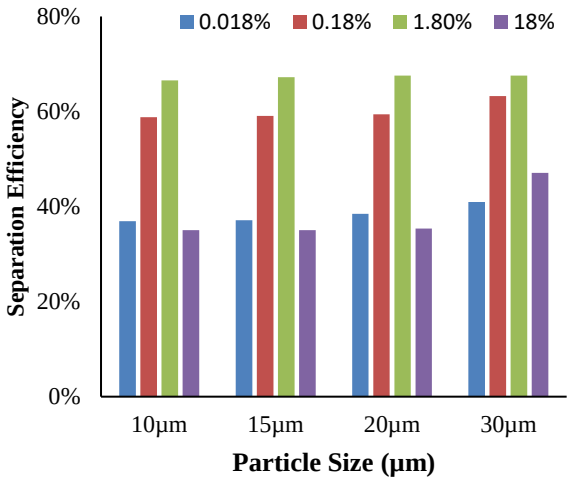

Fig. 4b: Magnetic Hydrocyclone.

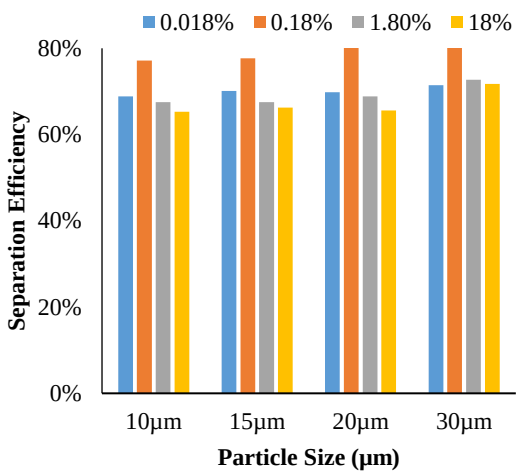

Fig. 4(a-b): Graph of Efficiency against Concentration.

4.3. Velocity Profile of liquid-liquid Hydrocyclone with Magnetic Particles

Figure 5-7 show radial variation of tangential, axial and radial velocities from the top wall of hydrocyclone for conventional and magnetic hydrocyclone. It can be seen from figure 5-7 that the use of magnetic particles increases all the velocity profiles (tangential, axial and radial).

4.3.1. Tangential Velocity (Figure 5)

Tangential velocity is found to be proportional to centrifugal force [27] [21], therefore it can be concluded that use of magnetic particle increases centrifugal force which leads to better separation of the dispersed phase. The change in particle density due to the addition of magnetic particles and the introduction of magnetic field are the main contributors to change in the velocity.

Irrespective of the flow in the cylindrical or conical part, tangential velocity shows characteristics of a forced vortex in the core region while the area from the wall to the maximum tangential velocity shows the characteristic of a free vortex. Free vortex is inversely proportional to radial length while forced vortex is directly proportional to radial length thus the change in graph shape along the radial axis. Higher tangential velocity in the free vortex facilitates particle movement to the wall while particles that enter into the core region (forced vortex region) are separated through the overflow. It is worthy to note that higher tangential velocity denotes higher swirling intensity.

4.3.2. Radial Velocity (Figure 6)

For particles to separate in cyclones, radial displacement must occur; figure 7 shows that radial velocity increases along the radial length and near the wall becomes zero due to the need for the total flow to pass through the smaller area as it leaves the cyclone. The negative value in radial velocity denotes inward radial velocity, this denotes the passage of fluid through to vortex finder and then becomes zero. The positive value is due to centrifugal force, (Wang B, et al, 2007).

Figure 6 showcase the radial velocity for conventional and magnetic hydrocyclone at the different axial location of Z=0.8Dc, 1.67Dc, and 3.33Dc. Radial velocity of magnetic hydrocyclone is higher than that of conventional hydrocyclone. Since radial velocity is proportional to drag force, it is deduced that the quantity of water expected at the overflow (in a magnetic cyclone) is greater than the quantity of oil at the overflow in a conventional cyclone.

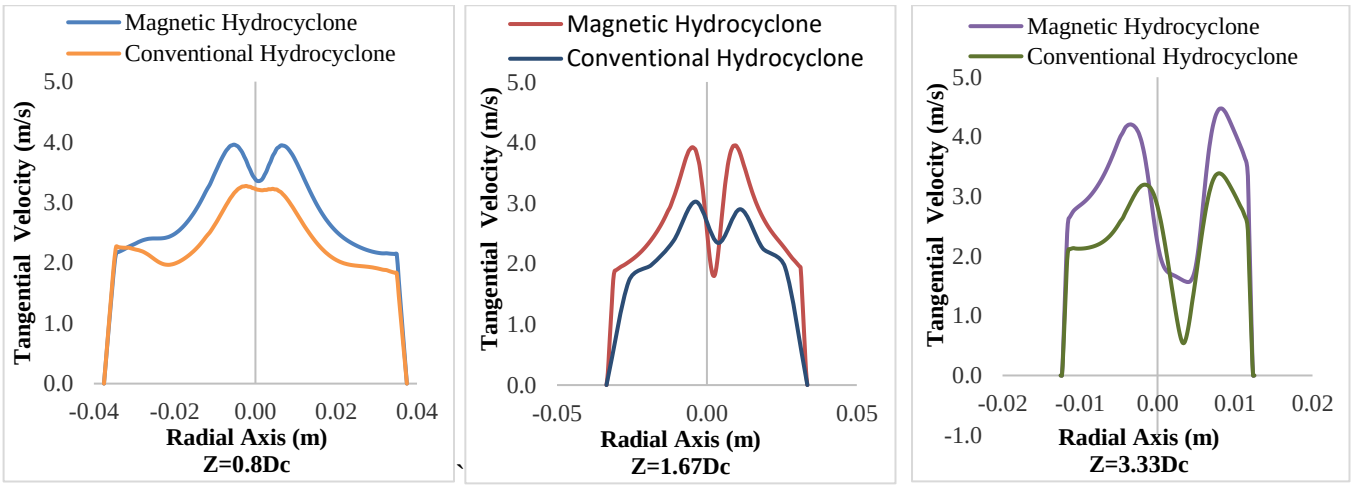

Fig. 5: Tangential Velocity of Magnetic and Conventional cyclone at different axial positions.

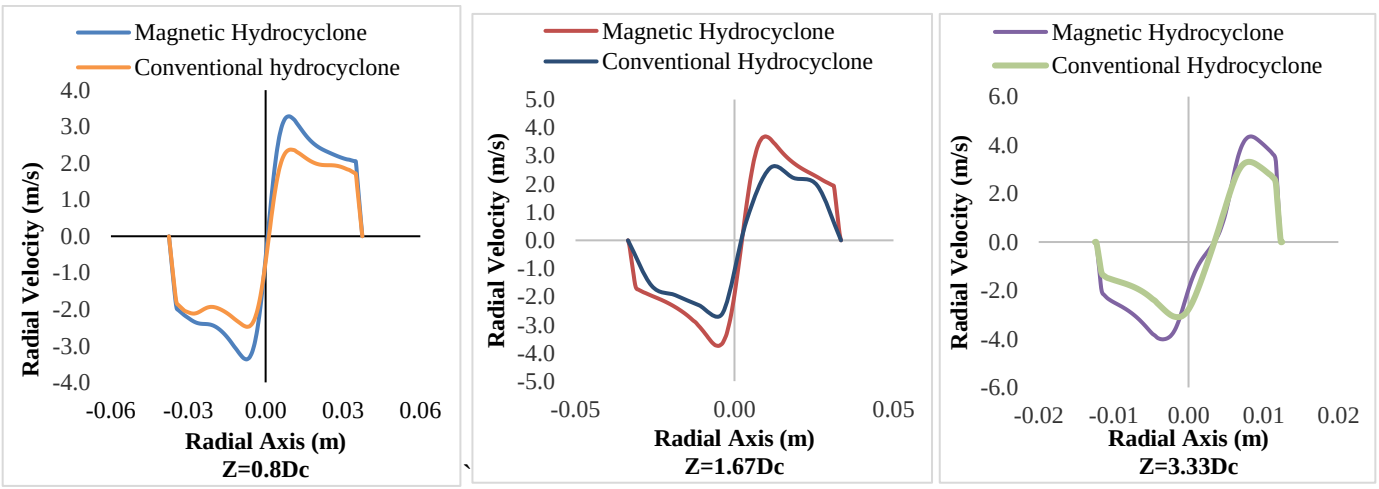

Fig. 6: Radial Velocity of Magnetic and Conventional Cyclone at different axial positions.

4.3.3. Axial Velocity (Figure 7)

Axial Velocity determines the separation zone or space, it acts towards the longitudinal axis of the cyclone. It is an important part of the cyclone flow field as it determines the residence time. The axial velocity is of two parts, the first part moves lower density fluid to overflow (positive) for magnetic and non-magnetic cyclones while the second part moves high-density fluid to the underflow (negative). The negative value in figure 7a implies at Z=0.8Dc, higher density fluid moves to the wall, Z=0.8Dc falls in the cylindrical section. And at Z=1.67Dc and Z=3.33Dc respectively (both in conical section), the lower density moves to the overflow. Since axial velocity determines the separation zone, the results show that most of the fine particle separation takes place in the conical section of the cyclone. It should also be noted that the axial velocity of conventional hydrocyclone increased when the magnetic particle was added implying a better separation of water from the overflow in magnetic hydrocyclone.

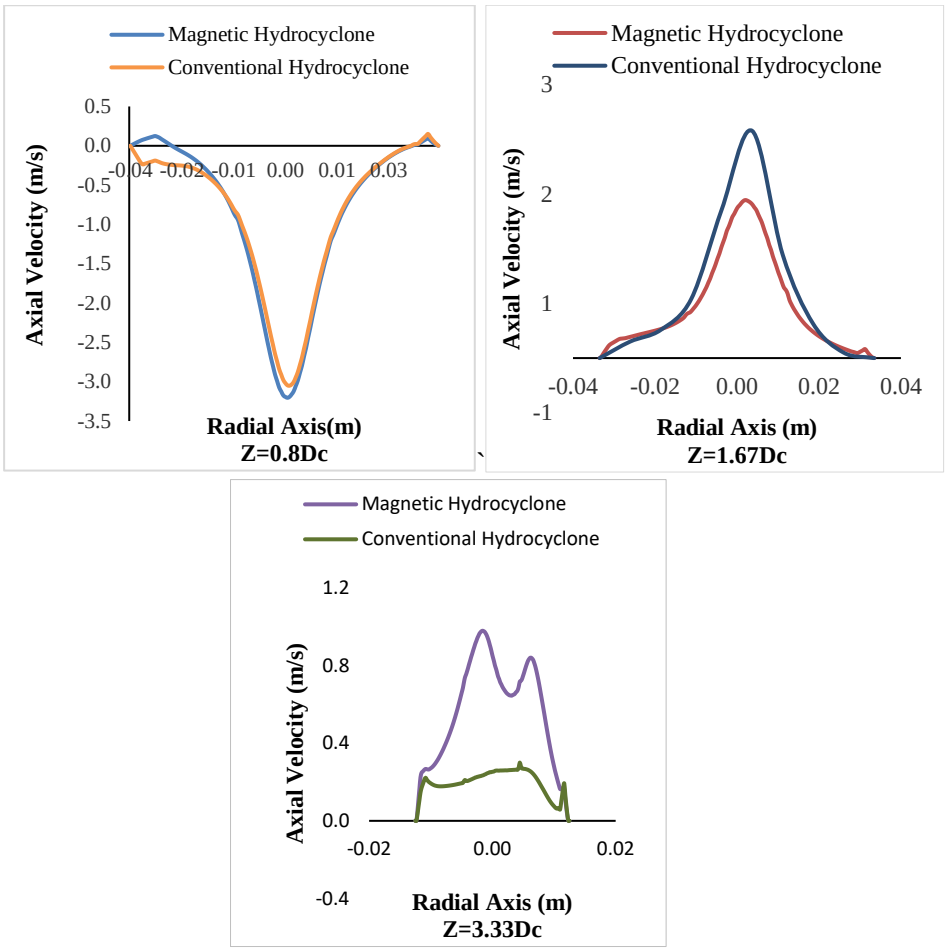

Fig. 7: Axial Velocity of Magnetic and Conventional Cyclone at different axial positions.

5. Conclusion.

The aim of the current research is to improve the separation efficiency of oil-water emulsion most especially 1-10µm droplet size. To achieve this micro-sized ferromagnetic particle mixed with a surfactant and doped with oil droplet is assumed to be feed into the cyclone (Watson design). The result showed an increase of 20-30% in separation efficiency for droplet size less than 10µm with the introduction of magnetic hydrocyclone and a further increase of about 1-4% when external magnetic field strength was increased from 0.5Tesla to 1.5Telsa. It was concluded that the efficiency increase mostly as a result of density differential introduced by the addition of ferromagnetic material and lightly by external magnetic field strength.

The use of magnetic particle also increased all the velocities in the flow (tangential, radial and axial velocity), and optimal efficiency was achieved at lower concentration when compared to a conventional cyclone.

References

[1] J. L. B. P. C. Arthur, “Technical summary of oil & gas produced water treatment technologies.,” All Consulting, LLC, Tulsa, OK, 2005.

[2] J. S. Souza, M. K. N. Paiva, F. P. M. Farias, S. R. Farias Neto and A. G. B. Lima, “Hydrocyclone applications in produced water: a steady-state numerical analysis,” *Brazilian Journal of Petroleum and Gas,* vol. 6, no. 3, pp. 133-143, 2012.

[3] Z.-s. Bai, H.-l. Wang and S.-T. Tu, "Oil-water separation using hydrocyclones enhanced by air bubbles," *Chemical Engineering Research and Design,* vol. 89, no. 1, pp. 55-59, 2011.

[4] S. Noroozi and S. H. Hashemabadi, “CFD simulation of inlet design effect on deoiling hydrocyclone separation efficiency,” *Chemical Engineering & Technology: Industrial Chemistry-Plant Equipment-Process Engineering-Biotechnology,* vol. 32, no. 12, pp. 1885-1893, 2009.

[5] L. G. Vieira, B. C. Silvério, J. J. Damasceno and M. A. Barrozo, “Performance of hydrocyclones with different geometries,” *The Canadian Journal of Chemical Engineering,* vol. 89, no. 4, pp. 655-662, 2011.

[6] Ş. Erikli and A. Olcay, “Inlet Diameter and Flow Volume Effects on Separation and Energy Efficiency of Hydrocyclones,” in *IOP Conference Series: Materials Science and Engineering* , 2015.

[7] M. Saidi, R. Maddahian and B. Farhanieh, “Numerical investigation of cone angle effect on the flow field and separation efficiency of deoiling hydrocyclones,” *Heat and Mass Transfer,* vol. 49, no. 2, pp. 247-260, 2013.

[8] F. Farias, J. Souza, W. Lima, A. Macêdo, S. Neto and A. Lima, “Influence of Geometric Parameters of the hydrocyclone and sand concentration on the water/sand/heavy-oil separation process: Modeling and Simulation,” *The International Journal of Multiphysics,* vol. 5, no. 3, pp. 187-202, 2011.

[9] S. H. H. &. A. J. C. S. Noroozi, “Numerical Analysis of Drops Coalescence and Breakage Effects on De-Oiling Hydrocyclone Performance,” *Separation Science and Technology,* vol. 48, p. 991–1002 , 2013.

[10] T. Neesse, J. Dueck, H. Schwemmer and M. Farghaly, “Using a high pressure hydrocyclone for solids classification in the submicron range,” *Minerals Engineering,* vol. 71, pp. 85-88, 2015.

[11] M. Ghodrat, S. Kuang, A. Yu, A. Vince, G. Barnett and P. Barnett, “Computational study of the multiphase flow and performance of hydrocyclones: effects of cyclone size and spigot diameter,” *Industrial & Engineering Chemistry Research,* vol. 52, no. 45, pp. 16019-16031, 2013.

[12] A. Motin and A. Bénard, "Design of liquid-liquid separation hydrocyclones using parabolic and hyperbolic swirl chambers for efficiency enhancement," *Chemical Engineering Research and Design,* vol. 122, pp. 184-197, 2017.

[13] M. Siadaty, S. Kheradmand and F. Ghadiri, “Improvement of the cyclone separation efficiency with a magnetic field,” *Journal of Aerosol Science,* vol. 114, pp. 219-232 , 2017.

[14] W. P. a. N. ROWSON, “Development of a Magnetic Hydrocyclone Separation for the Recovery of Titanium From Beach Sands,” *Physical Separation in Science and Engineering,* vol. 12, no. 4, pp. 215–222 , 2003.

[15] G. Shen, “Design and Analysis of Magnetic Hydrocyclones,” McGill University Libraries , 1989.

[16] R. Freeman, N. Rowson, T. Veasey and I. Harris, “The development of a magnetic hydrocyclone for processing finely-ground magnetite,” *IEEE Transactions on Magnetics,* vol. 30, no. 6, pp. 4665-4667, 1994.

[17] P.-p. Fan, H.-t. Peng and M.-q. Fan, “Using a permanent magnetic field to manipulate the separation effect of a dense medium cyclone,” *Separation Science and Technology,* vol. 51, no. 11, pp. 1913-1923, 2016.

[18] S. Mirshahghassemi, A. D. Ebner, B. Cai and J. R. Lead, “Application of high gradient magnetic separation for oil remediation using polymer-coated magnetic nanoparticles,” *Separation and Purification Technology,* vol. 179, pp. 328-334, 2017.

[19] J. Liu, H. Wang, X. Li, W. Jia, Y. Zhao and S. Ren, "Recyclable magnetic graphene oxide for rapid and efficient demulsification of crude oil-in-water emulsion," *Fuel,* vol. 189, pp. 79-87, 2017.

[20] P. H. J. V. A. S. Riele Paul Marie te, "Method For Separating a Fluid From a Mixture of Fluids Using Ferromagnetic Nanoparticles -". EUROPEAN PATENT OFFICE Patent EP2731114 A1, 14 05 2014.

[21] L. Ji, S. Kuang, Z. Qi, Y. Wang, J. Chen and A. Yu, "Computational analysis and optimization of hydrocyclone size to mitigate adverse effect of particle density," *Separation and Purification Technology,* vol. 174, pp. 251-263, 2017.

[22] Y. Zhang, P. Cai, F. Jiang, K. Dong, Y. Jiang and B. Wang, "Understanding the separation of particles in a hydrocyclone by force analysis," *Powder Technology,* vol. 322, pp. 471-489, 2017.

[23] M. Zahn, T. A. Hatton and S. R. Khushrushahi, "Magnetic colloid petroleum oil spill clean-up of ocean surface, depth, and shore regions". UNITED STATES OF AMERICA Patent US8945393B2, 03 02 2015.

[24] K.-T. Hsieh and K. Rajamani, "Phenomenological model of the hydrocyclone: Model development and verification for single-phase flow," *International Journal of Mineral Processing,* vol. 22, no. 1-4, pp. 223-237, 1988.

[25] G. Zhu and J.-L. Liow, "Experimental study of particle separation and the fishhook effect in a mini-hydrocyclone," *Chemical engineering science,* vol. 111, pp. 94-105, 2014.

[26] R. Sabbagh, M. G. Lipsett, C. R. Koch and D. S. Nobes, "Predicting equivalent settling area factor in hydrocyclones; a method for determining tangential velocity profile," *Separation and Purification Technology,* vol. 163, pp. 341-351, 2016.

[27] M. Shi, Y. Ruan, J. Li, Z. Ye, G. Liu and S. Zhu, "Numerical study of dense solid-liquid flow in hydrodynamic vortex separator applied in recirculating biofloc technology system," *Aquacultural Engineering,* vol. 79, pp. 24-34, 2017.